

Effects of CSR Generated from Upstream Bends in a Laser Plasma Storage Ring

C. Mitchell, J. Qiang, and M. Venturini

August 28, 2013

1 Introduction

The recent proposal [1] of a Laser Plasma Storage Ring (LPSR) envisions the use of a laser-plasma (LP) acceleration module to inject an electron beam into a compact 500 MeV storage ring. Electron bunches generated by LP methods are naturally very short (tens of femtoseconds), presenting peak currents on the order of 10 kA or higher. Of obvious concern is the impact of collective effects and in particular Coherent Synchrotron Radiation (CSR) on the beam dynamics in the storage ring. Available simulation codes (e.g. Elegant [2]) usually include transient CSR effects but neglect the contribution of radiation emitted from trailing magnets. In a compact storage ring, with dipole magnets close to each other, cross talking between different magnets could in principle be important. In this note we investigate this effect for the proposed LPSR and show that, in fact, this effect is relatively small. However our analysis also indicates that CSR effects in general would be quite strong and deserve a careful study.

2 Storage Ring Lattice

In this note, we investigate the CSR-induced energy kick experienced by a bunch as it propagates through one-quarter of the Laser-Plasma Storage Ring lattice illustrated in Fig. 1. The beam is assumed to propagate clockwise through the bends, which are numbered successively as $1, \dots, 8$. We will consider a 1-D model of longitudinal CSR in which the bunch propagates rigidly throughout the lattice. For the purpose of computing the longitudinal CSR wake, cavities and multipoles are treated as drifts of an equivalent length.

Within the indicated bend (Bend 1), a bunch will interact with CSR generated when its electrons lie upstream at their appropriate retarded times. In general, the dominant source of CSR in the indicated region will be the radiation generated within Bend 1. However, the bunch may also interact with radiation generated within Bends 7 and 8. This upstream CSR can follow the bunch through one or more lattice elements before finally interacting with the bunch. In this note, the significance of this effect is investigated using the 1-D CSR model of [3] together with an analytical

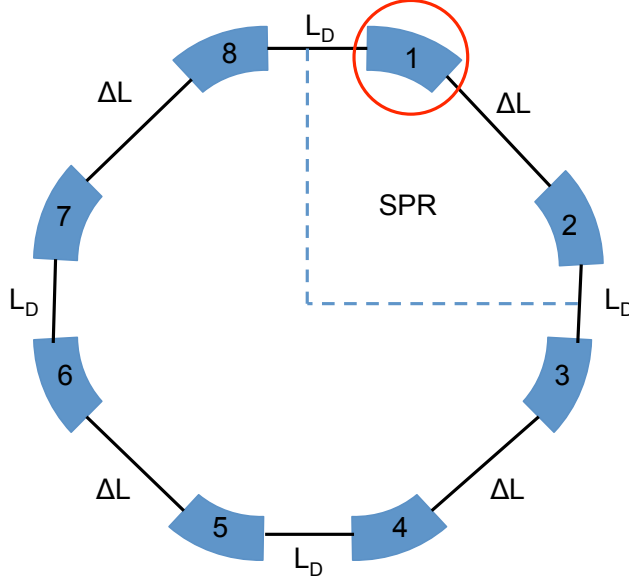


Figure 1: Geometry illustrating the proposed Laser-Plasma Storage Ring.

model of the longitudinal charge density in the storage ring, as described in the following section. The basic parameters describing the bunch and the relevant portion of the lattice are shown in Table 1.

Table 1: Parameters used for the Laser-Plasma Storage Ring.

E	0.5 GeV
I_{pk}	12 kA
Q_b	635 pC
ΔL	2.4 m
L_D	1.8 m
L_b	0.982 m
θ	0.785 rad

3 Model of the Bunch

The longitudinal phase space distribution for the bunch in the storage ring is shown in Fig. 2. The distribution is partitioned into two disconnected regions. The main body of the bunch, indicated by the macroparticles shown in red, contains a charge of 635 pC. The small region indicated in green contains a charge of 2.9 pC; for the purposes of this study, this portion is neglected. Neglecting this charge has negligible effect on the longitudinal current profile shown below.

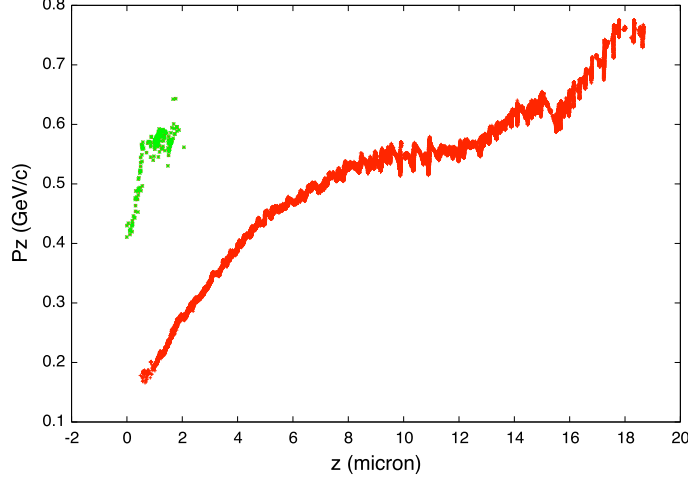


Figure 2: Longitudinal phase space for a bunch entering the storage ring.

The longitudinal density is modeled as:

$$\rho(z) = \frac{1}{L_b} \begin{cases} \rho_L(z), & -a - b \leq z < -a, \\ 1, & -a < z \leq a, \\ \rho_R(z), & a < z \leq a + r, \\ 0, & \text{otherwise.} \end{cases} \quad (1)$$

where

$$\rho_L(z) = \exp \left(1 - \frac{b^2}{b^2 - (z + a)^2} \right), \quad (2)$$

$$\rho_R(z) = \sqrt{r^2 - (z - a)^2} / r. \quad (3)$$

The density is uniquely described by the three length parameters a , b , and r , while the normalization L_b is determined from the requirement that

$$\int_{-\infty}^{\infty} \rho(z) dz = 1. \quad (4)$$

For a known peak current I_{pk} , the current profile along the bunch is given by:

$$I(z) = I_{pk} L_b \rho(z). \quad (5)$$

The relationship between the bunch charge and the peak current is determined by noting:

$$Q_b = \int_{-\infty}^{\infty} I(t) dt = \int_{-\infty}^{\infty} \frac{I(z)}{v_z} dz = \frac{I_{pk} L_b}{\beta c} \int_{-\infty}^{\infty} \rho(z) dz = \frac{I_{pk} L_b}{\beta c}. \quad (6)$$

A macroparticle distribution using 58623 particles for a bunch in the storage ring was used to obtain the longitudinal density profile along the bunch. This density profile was smoothed using a Bezier cubic spline, and the result was fitted against the analytical density profile (5). A fit given by the parameters $a = b = 4 \mu\text{m}$ and $r = 7 \mu\text{m}$ is shown in Fig. 3. These parameters give an rms bunch length of $\sigma_z = 5 \mu\text{m}$ and $L_b = 15.912 \mu\text{m}$. Using the fact that $Q_b = 635 \text{ pC}$ gives the peak current of $I_{pk} = 12 \text{ kA}$.

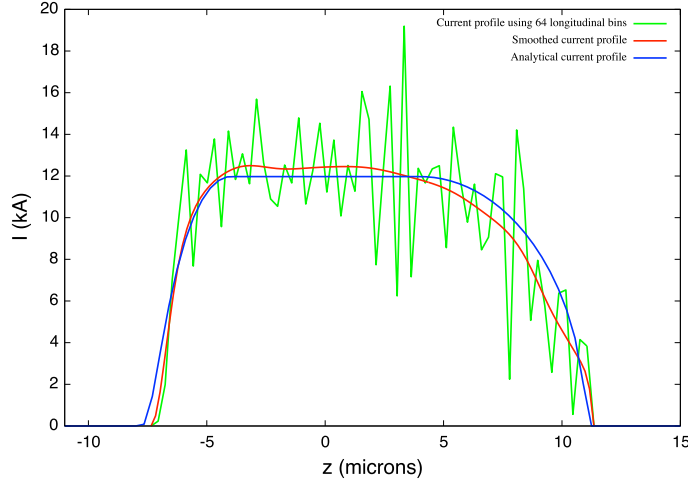


Figure 3: Comparison between the idealized current profile of (5) with $a = b = 4 \mu\text{m}$ and $r = 7 \mu\text{m}$ (blue), and the smoothed current profile obtained using the macroparticle distribution corresponding to Fig. 2 (red). The current profile with noise is shown in green, and the head of the bunch is located at $z = a + r = 11 \mu\text{m}$.

4 CSR Wakefields

4.1 Steady-state CSR

The free-space steady-state CSR wake generated within a single bend of the storage ring is illustrated in Fig. 4 (red), together with the current profile along the bunch (blue). The wake was computed using an integrated Green function method based on the 1-D CSR model of [3] together with the longitudinal charge density described in the previous section. In this regime, the steady-state wake is well-described by using an asymptotic approximation to the 1-D CSR kernel, since the short-range behavior of the CSR kernel occurs on the scale $R/\gamma^3 \ll \sigma_z$, where R is the bend radius. (See (19) of [4] and (17) of [3].)

4.2 Including transient effects

Figure 5 illustrates the free-space CSR wake along the length of the bunch at several different locations within Bend 1. The results shown include the effect of CSR generated within Bend 1, as well as within Bends 7 and 8, together with the transient fields that are produced when transitioning from a drift into a bend [3, 4]. In each case, the wake was computed using an integrated Green function method. Note that once the bunch has propagated 6 cm into the bend, the total CSR wake along the bunch is indistinguishable from the steady-state wake of Fig. 4.

Figure 6 illustrates the difference between the CSR wake of Fig. 5 and the CSR wake that is obtained when only entry transients [4] are included. Thus, Fig. 6 represents the contribution of Bends 7-8 to the total wake in Bend 1 (“upstream CSR”). This upstream CSR takes the shape

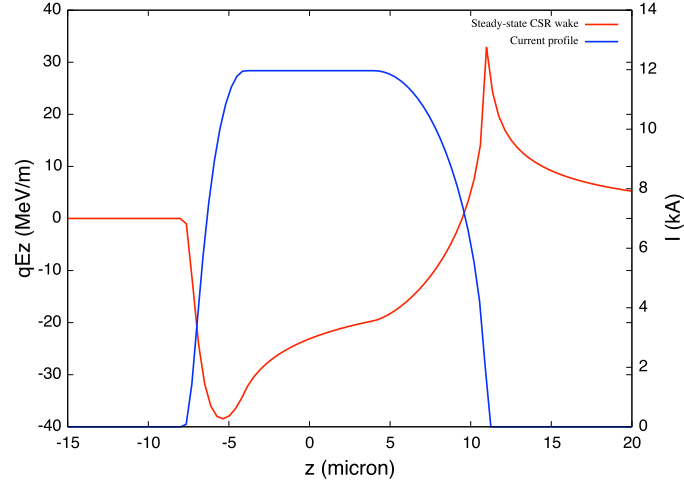


Figure 4: (Blue) Idealized current profile of the bunch. (Red) Steady-state CSR wake inside Bend 1. The head of the bunch is located at $z > 0$.

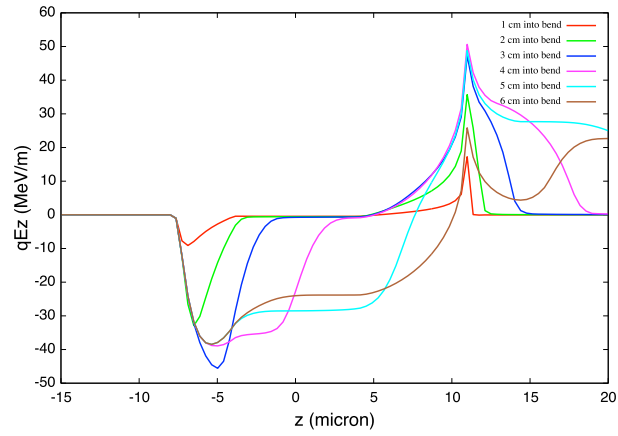


Figure 5: Total CSR wake when the bunch centroid is located at 1, 2, 3, 4, 5, and 6 cm into Bend 1.

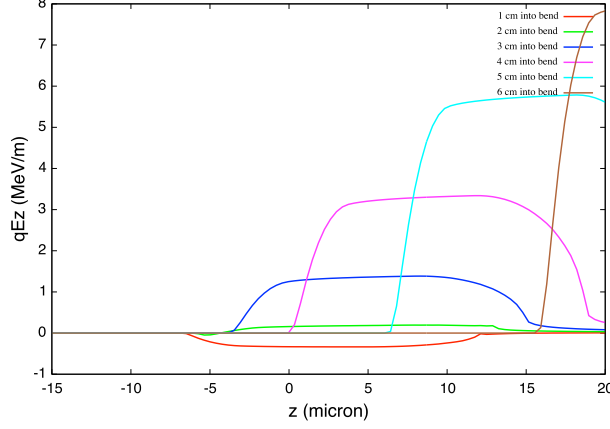


Figure 6: Upstream contribution from Bends 7, 8, and associated drifts to the CSR wake inside Bend 1. The difference between the CSR wake as computed with and without the effect of upstream bends is shown at 1, 2, \dots , 6 cm into the bend.

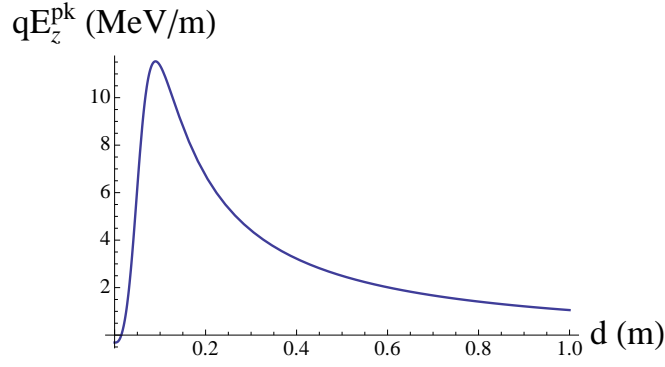


Figure 7: Peak value of the upstream contribution to the CSR wake as a function of distance into Bend 1.

of the longitudinal density of the bunch, with a centroid that shifts forward relative to the bunch centroid as the bunch moves downstream into the bend. The peak value of the upstream CSR wake is shown in Fig. 7 as a function of the distance d of the bunch centroid into Bend 1, and it reaches a maximum near $d = 10$ cm. Beyond 6 cm, there is negligible interaction between the bunch and the upstream CSR wake.

To better understand the interaction between the bunch and the CSR wake, note that the wake is given by an integral of the form:

$$W(z) = \int_{-\infty}^z K_{CSR}(z, z') \rho(z') dz', \quad (7)$$

where ρ denotes the longitudinal number density of the bunch, z denotes the longitudinal coordinate within the bunch, and K_{CSR} is the CSR interaction kernel [3]. Thus, a particle in the bunch at a longitudinal location z receives energy kicks from particles upstream in the bunch at locations $z' < z$. The kernel is typically shown as a function of the path length difference $\zeta = z - z'$. Particles that lie within a distance $0 \leq \zeta < \zeta_1$ of the observation point lie within Bend 1 at their retarded times. Particles that lie within a distance $\zeta_1 \leq \zeta < \zeta_2$ of the observation point lie within the drift

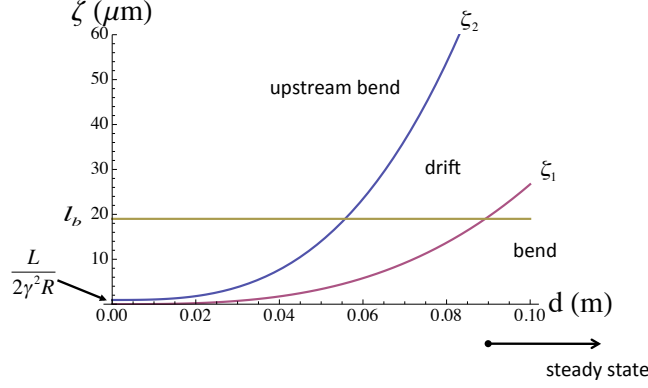


Figure 8: Quantities ζ_1 and ζ_2 , illustrating the relative contributions of upstream, transient, and steady-state CSR effects as a function of distance into Bend 1.

preceding Bend 1, and particles that satisfy $\zeta \geq \zeta_2$ lie within Bend 8 or beyond. Thus, the bunch upstream of a given location z is partitioned into three regions characterized by the parameters ζ_1 and ζ_2 . Figure 8 illustrates these quantities as a function of the distance d of the bunch centroid into Bend 1. Here l_b denotes the end-to-end length of the bunch. When $\zeta_2 > l_b$, there is no contribution from upstream CSR. Similarly, when $\zeta_1 > l_b$, there is no contribution from entry transient effects, and the CSR wake is identical to its steady-state value.

4.3 Energy kick

The net energy kick experienced by a particle in the bunch as it propagates through one-quarter of the storage ring was computed by integrating the CSR wake through the portion of the lattice indicated *SPR* in Fig. 1. The result is shown in Fig. 9. In the figure shown at left, the CSR wake within each element contains contributions from the two preceding bends, together with entry and exit transients.

The figure at right in Fig. 9 illustrates the difference between the energy kick that is obtained with and without the inclusion of upstream CSR, indicating that this difference is approximately 0.2% relative to the peak energy loss of 80 MeV. Note that the energy kick due to upstream CSR is very small due to the fact that the upstream CSR wake decouples from the bunch within the first 6 cm of the bend entry (Fig. 8).

5 Summary

A 1-D integrated Green function routine based on [3] was used to compute CSR wakefields in the Laser-Plasma storage ring of Fig. 1, using the idealized beam profile of (1). The effect of radiation from upstream bends is included. The short rms bunch length (5 μm) and large peak current (12 kA) result in strong CSR-induced energy loss near 1 GeV. However, the short bunch length also results in a rapid decoupling between the bunch and the effects of radiation from upstream bends. Results obtained using this idealized beam profile indicate that the CSR from upstream bends

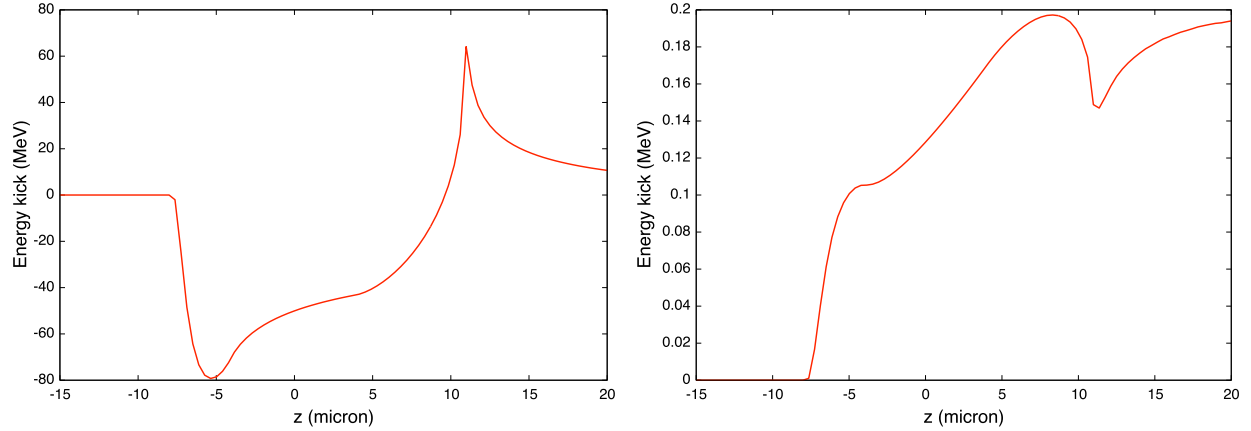


Figure 9: (Left) Net energy kick through one-quarter of the LPSR lattice, including the effect of CSR from upstream bends and associated drifts. (Right) Contribution from upstream bends to the CSR energy kick through one-quarter of the lattice.

contributes only 0.2% of the total energy kick experienced by particles in the storage ring. Note that the 1-D CSR model in ELEGANT does not include the effect of radiation from upstream bends, and neglecting this effect appears justified for the storage ring considered here.

6 Acknowledgements

This work made use of computer resources at the National Energy Research Scientific Computing Center and was supported by the U.S. Department of Energy under Contract No. DE-AC02-05CH11231.

References

- [1] K. Robinson et al., “Novel laser-plasma ring for synchrotron radiation and particle physics applications”, Private comm. (2012).
- [2] M. Borland, Advanced-Light Source LS-287, Sept. 2000.
- [3] D. Sagan et al., Phys. Rev. ST-AB, **12**, 040703 (2009).
- [4] E. L. Saldin et al., Nucl. Instr. and Meth. in Phys. Res. A **398**, 373-394 (1997).

This document was prepared as an account of work sponsored by the United States Government. While this document is believed to contain correct information, neither the United States Government nor any agency thereof, nor The Regents of the University of California, nor any of their employees, makes any warranty, express or implied, or assumes any legal responsibility for the accuracy, completeness, or usefulness of any information, apparatus, product, or process disclosed, or represents that its use would not infringe privately owned rights. Reference herein to any specific commercial product, process, or service by its trade name, trademark, manufacturer, or otherwise, does not necessarily constitute or imply its endorsement, recommendation, or favoring by the United States Government or any agency thereof, or The Regents of the University of California. The views and opinions of authors expressed herein do not necessarily state or reflect those of the United States Government or any agency thereof or The Regents of the University of California.